A&A 398, 1073–1079 (2003)
DOI: 10.1051/0004-6361:20021728

Astronomy & Astrophysics

Physical parameters of the Algol system BP Muscae from simultaneous analysis of GENEVA 7-colour light curves⋆,⋆⋆

F. Carrier, F. Barblan, G. Burki, P. Bartholdi, and B. Nicolet

Observatoire de Genève, 51 chemin des Maillettes, 1290 Sauverny, Switzerland

Received 3 September 2002/ Accepted 6 November 2002

Abstract. The semi-detached eclipsing binary system BP Muscae has been analysed using the Wilson-Devinney program. Light curves have been obtained in the GENEVA 7-colour photometric system, and radial velocity curves for both components have been measured with the spectrograph CORALIE. The physical and orbital parameters have been determined through a self-consistent simultaneous solution of light curves in seven colours and of the radial velocity curves of both components. The absolute elements of the components are, for the primary (mass gainer), $M_1 = 2.40 \pm 0.01\ M_\odot$, $R_1 = 2.64 \pm 0.01\ R_\odot$, $M_{\mathrm{bol}_1} = 0.66 \pm 0.04$, $T_{\mathrm{eff}_1} = 9180 \pm 90$ K, and for the secondary (mass loser), $M_2 = 0.68 \pm 0.01\ M_\odot$, $R_2 = 3.76\ R_\odot$, $M_{\mathrm{bol}_2} = 2.40 \pm 0.08$, $T_{\mathrm{eff}_2} = 5160 \pm 90$ K. The semi-major axis A of the relative orbit is $13.617 \pm 0.019\ R_\odot$. The spectral type of the components are A0.5/1.5 V (primary) and about G5 III. The distance to BP Mus is evaluated as 562 ± 17 pc, and the colour excess *E[B2-V1]* as 0.220 ± 0.014.

Key words. stars: individual: BP Muscae – stars: binaries: eclipsing – stars: binaries: close – stars: fundamental parameters – techniques: photometric – techniques: radial velocities

1. Introduction

BP Muscae (CD −71°884, CPD −71°1392) is a semi-detached eclipsing binary of period $P = 3.320$ days, with an evolved secondary component. The total primary eclipse is 2.75 mag deep in the V band. The variability of BP Mus was discovered by Hoffmeister (1943), who derived a first estimate of the period and established an Algol type light curve. The system was monitored in *UBV* photometry by Kviz (1986), who made a raw estimate of the spectral types of the components from the colours, A5 V and K2 III. This classification is not completely confirmed by the detailed analysis made in this paper, which gives A0.5/1.5 V for the primary and about G5 III for the secondary.

Very little is known about BP Mus. In particular, no complete light or radial velocity curves have been published yet. For that reason, this star was measured intensively in the 7-colour GENEVA photometric system (Golay 1980; Rufener 1988) using the 0.70 m Swiss telescope at La Silla (European Southern Observatory, Chile) equipped with the two-channel aperture photometer P7 (Burnet & Rufener 1979). Moreover, the radial velocity curve of both components has been determined with the spectrovelocimeter CORALIE installed on the 1.20 m Swiss telescope at La Silla.

In this paper, the physical parameters of the two components of this eclipsing system will be determined from the simultaneous analysis of the light and radial velocity curves.

2. Period

The orbital period listed in the GCVS (Kholopov 1985), $P = 3.32058$ days, is the value derived by Hoffmeister (1943) in 1936–1938. A slightly shorter value, 3.32046 d, was obtained by Kviz (1986) in 1978–1979. On the basis of this too limited number of determinations, it was not possible to make an extensive analysis of possible variation of the orbital period. A new and independant determination of the ephemeris was made on the basis of our photometric survey. From 1984 to 1991, no significant variation of the period was noted, and the adopted ephemeris is :

$$\mathrm{HJD(Min\ I)} = (2\,446\,415.1700 \pm \mathit{0.0010}) + (3.3204949 \pm \mathit{0.0000040}) \times E. \quad (1)$$

The uncertainty on the period corresponds to an error of 0.001 in phase over the 2707 days of the surveys (815·P).

The comparison of these values with those resulting from the calculation of the orbital motion (see Table 4 and Fig. 1 in Sect. 5) shows a difference $\Delta\phi = 0.00671$ in phase between the center of the primary eclipse (photometry) and the passage at the systemic velocity, when the velocity of the secondary is

Send offprint requests to: F. Carrier,
e-mail: `Fabien.Carrier@obs.unige.ch`

⋆ Based on observations collected at the Swiss 70 cm and 120 cm telescopes at the European Southern Observatory (La Silla, Chile).

⋆⋆ Table 1 is only available in electronic form at the CDS via anonymous ftp to `cdsarc.u-strasbg.fr (130.79.128.5)` or via `http://cdsweb.u-strasbg.fr/cgi-bin/qcat?J/A+A/398/1073`

Table 2. The seven mean GENEVA apparent magnitudes of BP Mus, with the uncertainties. In parenthesis (column secondary) is given the value of the uncertainties which ought to have resulted from a "normal" integration time of the measurements, i.e. 12 min (normal) instead of 6 min (during the primary eclipse).

Mag	BP Mus A+B Observed	Secondary Observed		Primary Calculated
U	11.302 ± 0.022	15.930 ± 0.210	(0.150)	11.317 ± 0.025
$B1$	10.551 ± 0.016	14.983 ± 0.062	(0.044)	10.570 ± 0.017
B	9.588 ± 0.012	13.562 ± 0.030	(0.021)	9.616 ± 0.013
$B2$	11.002 ± 0.013	14.638 ± 0.052	(0.037)	11.041 ± 0.015
$V1$	10.861 ± 0.009	13.695 ± 0.044	(0.031)	10.944 ± 0.013
V	10.140 ± 0.008	12.908 ± 0.009	(0.006)	10.228 ± 0.009
G	11.238 ± 0.011	13.780 ± 0.034	(0.024)	11.348 ± 0.016

increasing (radial velocity). This difference can be easily explained by a small variation of the period between the two epochs of our measurements (1984–1991 for the photometry, 1999 for the radial velocities).

3. Photometric data and variability of the components

GENEVA 7-colour photometric measurements of BP Muscae were obtained from Jan. 06, 1984 to Jun. 05, 1991, using the Swiss 70 cm telescope at the European Southern Observatory (ESO), La Silla, Chile. During this period, 373 measurements of weight $q \geq 1$ have been obtained (see Rufener 1988, for the definition of the weight q). These data are listed in Table 1.

The magnitudes in each of the seven filters are obtained from the visual magnitude V and the six colour indices in the following manner:

$$i = V - [V - B] + [i - B] \quad (2)$$

with i representing one of the seven filters $U, B, V, B1, B2, V1, G$. It is possible to calculate the magnitude of the primary (mass gainer) by subtracting the flux of the secondary (mass loser), at the bottom of the total primary eclipse, from the flux of the both components measured together (outside the eclipses). This calculation has been made for each of the 7 GENEVA magnitudes and the results are given in Table 2, with the uncertainties.

It is interesting to compare the observed uncertainties with the mean precision of the measurements made in GENEVA photometry. Rufener (1988, Fig. 2) has shown the shape of the mean relation σ_V vs. V obtained for the non-variable stars, in particular the progressive increase of σ_V with increasing V, for stars fainter than $V \simeq 9$.

From the values in Table 2 and the relation given by Barblan et al. (1998, Fig. 2), it appears that the uncertainties on the measurements of BP Mus are in agreement with the expected precision of the measurements, with only one exception: the dispersion of the measurements in the band U is rather large, by a factor 1.5, outside the eclipses, (i.e. in the case BP Mus A+B, see Table 2), and thus affects primary values, too. This could be due to a variable disk around the mass gainer.

4. Classification of the components and interstellar extinction

A photometric classification of the components of BP Mus can be obtained by using the general properties of the GENEVA photometric system. The same method has been applied to the analysis of two other eclipsing systems, RZ Eridani (Burki et al. 1992) and TZ Eridani (Barblan et al. 1998). Our analysis is based on the technique of the *photometric boxes* (Golay et al. 1969; Nicolet 1981a), in which it is assumed that the stars that have the same photometric reddening-free parameters as the primary of BP Mus are intrinsically similar to it (twin stars). These parameters, i.e. d, Δ and g (e.g. Golay 1980), have been calculated from the magnitudes given in Table 2.

The entire GENEVA photometric database, which contains roughly 48 000 stars, has been searched for stars very similar to BP Mus A. With the value 0.015 mag for the radius of the photometric box on the parameters d, Δ and g, 67 twin stars have been found, of which 9 belong to open clusters having well determined values of distance and interstellar reddening by Nicolet (1981b). This is of course a necessary condition to derive the photometric parameters of BP Mus A. These 9 twin stars belong to NGC 2287, NGC 3532, NGC 6633, NGC 6281 (2 stars in each cluster) and NGC 7092.

From the mean intrinsic colours of these twin stars in open clusters, we derive for the primary of BP Mus: $[B2 - V1]_0 = -0.123 \pm 0.012$. According to the relations between spectral types and intrinsic GENEVA colours or parameters by Hauck (1994) and to the calibration of GENEVA photometry based on Kurucz's atmosphere models by Künzli et al. (1997), a first estimate of the parameters of the primary can be given: A0.5/1.5 V for the spectral type, 9180 ± 90 K for the effective temperature, $\log g = 4.14 \pm 0.10$ for the mean surface gravity (for a solar metallicity). On the other hand, the estimated colour excess is $E[B2 - V1] = 0.220 \pm 0.014$.

For the secondary, the intrinsic colours have been calculated by using the measured values (see Table 2) and the colour excesses obtained for the primary. We derived in particular $[B2 - V1]_0 = 0.72 \pm 0.11$, an estimated spectral type of G9/K0 III (±2 subclasses) and an effective temperature of 4600 ± 300 K. This estimate is imprecise, due to the faintness of the secondary component. The values obtained by the analysis of the eclipsing system are certainly better, i.e. 5157 ± 23 K and G5III (see Sect. 6).

Table 3. Journal of the radial velocity observations of BP Mus. The phases are computed by using the data given in Table 4.

HJD −2 451 200	$V_r \pm \sigma$ (A) [km s^{-1}]		$V_r \pm \sigma$ (B) [km s^{-1}]		phase
27.8039	−50.40	0.78	93.22	3.03	0.3792
28.8642	25.54	0.72	−166.02	2.06	0.6986
29.7649	8.59	1.62	−44.24	2.75	0.9698
30.8363	−62.48	0.60	129.66	1.95	0.2925
31.7220	−0.36	1.71	−78.33	3.37	0.5592
32.8053	13.55	0.83	−123.65	2.51	0.8855
33.7291	−58.20	0.71	113.57	1.74	0.1637
34.8257	−24.95	1.78	-	-	0.4939
35.6369	27.70	1.25	−177.11	2.56	0.7382
35.8352	28.57	0.76	−169.89	1.97	0.7979
36.6392	−40.19	1.67	18.55	3.61	0.0401
36.8731	−50.02	0.89	85.55	2.30	0.1105
37.8934	−42.11	1.90	61.10	3.89	0.4178
38.6218	16.48	0.98	−139.46	2.59	0.6372
39.8249	-	-	−17.53	1.65	0.9995
40.8759	−62.27	0.73	125.65	2.53	0.3160
41.8355	11.74	0.94	−115.09	3.23	0.6050
42.8786	5.87	1.90	−91.54	4.25	0.9191
43.7764	−63.67	0.80	130.61	2.19	0.1895
43.8911	−62.77	2.41	139.24	5.95	0.2241
43.9069	−63.40	1.09	134.42	3.45	0.2288
44.8794	−15.21	2.04	-	-	0.5217
45.8530	24.02	0.90	−158.58	2.20	0.8149

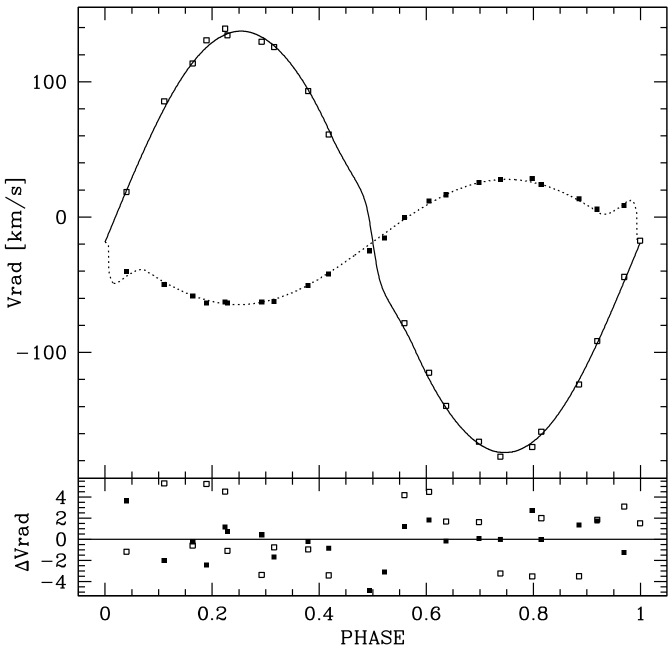

Fig. 1. Radial velocity curve and residuals of BP Mus. The black squares refer to the primary component, and the open squares to the secondary. The adjusted curves result from the solution of the Wilson-Devinney program, based on the simultaneous photometric and radial velocity analysis (see Sect. 6).

5. Radial velocity curves

BP Mus was observed over a campaign of more than two weeks (18 February–8 March 1999) with the Coralie high-resolution fiber-fed echelle spectrograph (Queloz et al. 2001) mounted on the Nasmyth focus on the 120 cm Swiss telescope at La Silla (ESO, Chile). Coralie reaches, with a 3 pixel sampling, a resolving power of 50 000 ($\lambda/\Delta\lambda$). Coralie data were reduced at the telescope, using a software package called INTER-TACOS (INTERpreter for the Treatment, the Analysis and the COrrelation of Spectra), developed by D. Queloz and L. Weber at the Geneva Observatory (Baranne et al. 1996). 22 echelle-spectra were obtained during the survey. These observations cover 68 orders in the spectral range 3875–6820 Å. S/N ratios of spectra vary from 20 to 45 at 6000 Å.

Radial velocities were obtained by cross-correlation between the considered spectrum and a reference mask. It is important to use a template as similar as possible to the real spectrum. Thus, two different masks were build from synthetic spectra to determine the radial velocities of the primary and secondary (spectral type A and G respectively). The spectrum synthesis of the spectral region 3875–6820 Å was accomplished using the SYNSPEC (Hubeny et al. 1994) code with ATLAS9 model atmospheres interpolated from Kurucz grid (1994). The Vienna Atomic Line Database (VALD-2) was used to create a line list for the spectrum synthesis (Kupka et al. 1999). First a synthetic spectrum is computed without rotation, with a solar composition and with a microturbulent velocity of 2 km s^{-1}. Next this spectrum is broadened with profiles to take the rotation and the resolving power of the observed spectra into account. Many tests were conducted employing several templates to discover which yielded the strongest and sharpest cross-correlation function. The radial velocities were finally obtained by fitting the cross-correlation function with two Gaussians. The radial velocities using A5- and K0-type masks were adopted respectively for the primary and the secondary.

The log of the radial velocity observations is given in Table 3 and the radial velocity curve is shown in Fig. 1. The mass ratio is well constrained through the radial velocity measurements ($q = 0.299 \pm 0.008$). The sharp discontinuity due to the partial eclipse of a rotating star (the Rossiter effect) is seen at phase zero. The orbital elements are given in Table 4.

6. Photometric solution

The photometric solution for BP Mus eclipses was obtained with the Wilson-Devinney WD program (Wilson & Devinney 1971; Wilson 1992), using the version revised in 1995. We used the WD program in Mode 5, adapted for semi-detached systems, allowing a simultaneous computation on the light curves in the Geneva photometric system, based on 373 measurements (see Sect. 3), and the radial velocity curves of both components (see Sect. 5). Some tests have been made using the WD program in Mode 2, used in the case of a detached system. The similarities of the results, in particular on the radius r_{point_2} (see Table 7), is confirmation that BP Mus is a semi-detached Algol system, thus lobe filling of the cool losing component was assumed. The procedure followed to find the best solution was globaly described by Barblan et al. (1998). Only the main points are given here for the case of BP Mus.

Table 4. Orbital elements of the binary system, based on the radial velocity analysis. For each component, the second line gives the estimated standard deviations of the parameters. The period has been fixed to the photometric value.

Star name	P [days]	$T_\circ$ [HJD −2 400 000]	e	$V_\circ$ [km s^{-1}]	ω_1 [°]	$K_{1,2}$ [km s^{-1}]	$M_{1,2}\sin^3 i$ [$M_\odot$]	$a_{1,2}\sin i$ [10^6 km]	N	(O–C) [km s^{-1}]
BP Mus A	3.3204949	51233.1858	0.000	−18.37	–	47.06	2.254	2.149	22	1.47
	fixed	0.0028	fixed	0.31	–	0.45	0.028	0.021		
BP Mus B	3.3204949	51233.1858	0.000	−18.37	–	157.00	0.676	7.169	21	2.58
	fixed	0.0028	fixed	0.31	–	0.74	0.010	0.034		

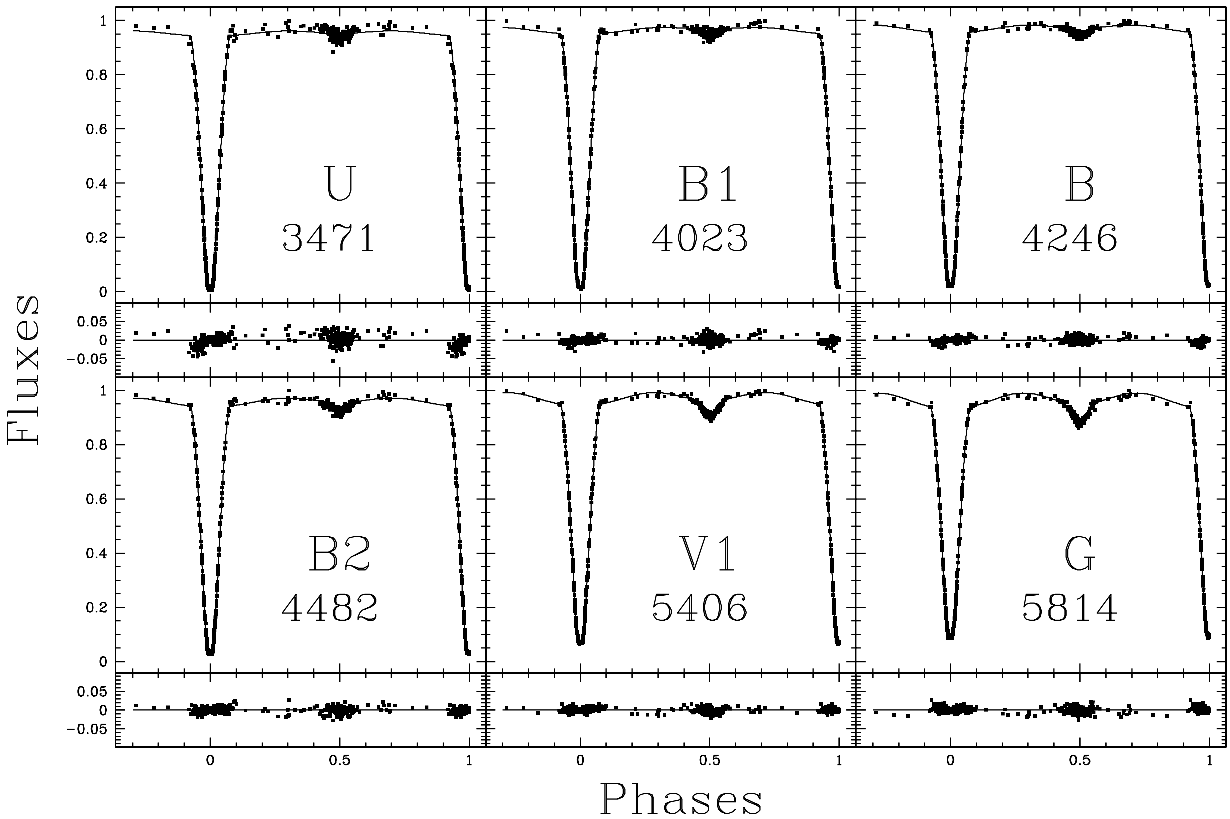

Fig. 2. Light curves of BP Mus in 6 of the 7 Geneva photometric passbands (*U, B1, B, B2, V1, G*). The light curve in *V* is given in Fig. 3.

The following parameters have fixed values:

- The primary temperature $T_1 = 9180$ K.
- The bolometric albedos, taken at the theoretical values $A_1 = 1.0$ (radiative case) and $A_2 = 0.5$ (convective case.
- For both primary and secondary components, a logarithmic limb-darkening law of the form:

  $$I = I_0(1 - x + x\cos\theta - y\cos\theta\ln(\cos\theta)) \quad (3)$$

  was assumed (van Hamme 1993). For the secondary, both x and y parameters were fixed to their theoretical values, interpolated from Table 2 of van Hamme (1993). Indeed, the secondary minimum is too shallow to allow the determination of x_2. The adopted values of y_1, x_2 and y_2 and the adjusted values of x_1 are listed in Table 5.
- The exponent g of the gravity darkening law, taken equal to 1.00 for the primary (radiative case, see Wilson & Biermann 1976).
- The orbital eccentricity $e = 0$.

Table 5. Logarithmic limb-darkening parameters x and y.

Passband	y_1 fixed	x_2 fixed	y_2 fixed	x_1 adjusted (except U)	
U	0.240	0.856	−0.299	0.572	
B1	0.325	0.854	−0.021	0.795	±0.008
B	0.325	0.854	−0.021	0.775	±0.006
B2	0.325	0.854	−0.021	0.765	±0.007
V1	0.287	0.801	0.131	0.599	±0.007
V	0.287	0.801	0.131	0.595	±0.007
G	0.287	0.801	0.131	0.578	±0.010

The other characteristics of the parameters necessary to the calculations are: i) the grid resolution values were taken as 30, 30, 30, 30 for N1, N2, N1L and N2L respectively (see WD program); ii) for both components, the stellar atmosphere models of Kurucz (1994) integrated through the Geneva photometry passbands (Rufener & Nicolet 1988) have been used.

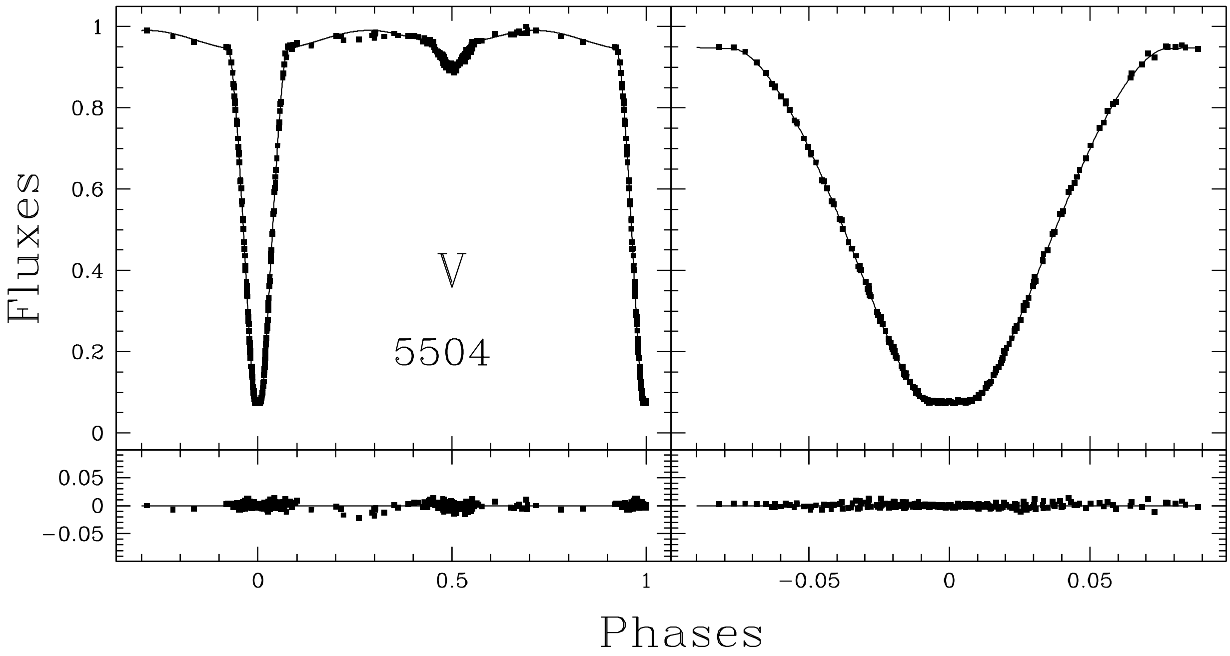

Fig. 3. The light curve of BP Mus in magnitude V, with an enlargement of the primary eclipse.

Table 6. Adjusted parameters of the system BP Mus from the Wilson-Devinney program. Indices 1 and 2 refer to the primary (hot) and secondary (cool) components. The primary temperature T_1 is fixed to 9180 K.

T_2 [K]	5157	±23
A [$R_\odot$]	13.617	±0.019
i [°]	87.02	±0.02
$q = M_2/M_1$	0.2840	±0.0004
Ω_1	5.450	±0.006
Ω_2	2.43	
g_2	0.644	±0.005
$L_1/(L_1 + L_2)$		
U	0.9819	±0.0019
$B1$	0.9772	±0.0002
B	0.9642	±0.0002
$B2$	0.9517	±0.0002
$V1$	0.9010	±0.0002
V	0.8930	±0.0002
G	0.8692	±0.0003
$L_2/(L_1 + L_2)$		
U	0.0181	±0.0019
$B1$	0.0228	±0.0002
B	0.0358	±0.0002
$B2$	0.0483	±0.0002
$V1$	0.0990	±0.0002
V	0.1070	±0.0002
G	0.1308	±0.0003

Table 7. Computed parameters of the system BP Mus. Indices 1 and 2 refer to the primary (hot) and secondary (cool) components.

M_1 [$M_\odot$]	2.40	±0.01
M_2	0.68	±0.01
R_1 [$R_\odot$]	2.64	±0.01
R_2	3.76	
$\log g_1$	3.97	±0.01
$\log g_2$	3.12	
M_{bol_1}	0.66	±0.04
M_{bol_2}	2.40	±0.08
r_{pole_1} [A]	0.1934	±0.0002
r_{point_1}	0.1950	±0.0002
r_{side_1}	0.1943	±0.0002
r_{back_1}	0.1948	±0.0002
r_{pole_2} [A]	0.2572	±0.0001
r_{point_2}	0.3737	±0.0005
r_{side_2}	0.2678	±0.0001
r_{back_2}	0.3004	±0.0001

The adjustable parameters are the semi-major axis A, inclination i, cool star temperature T_2, hot and cool star luminosities L_1 and L_2 in each passband, hot star limb darkening coefficient x_1, cool star gravity darkening exponent g_2 and potential Ω_1 at the hot star surface. The value of the potential Ω_2 is determined by the semi-detached solution. Recall that Ω is a non-dimensional parameter that is a linear function of the true potential Ψ (Kopal 1959; Wilson & Devinney 1971).

No satisfying solution was obtained when the U light curve was included. This could be due to the following reasons: i) the U luminosity is very faint during the primary eclipse, thus the precision is insufficient and biases the whole adjustment; ii) the U luminosity is affected by a physical effect which is not taken into account by the WD program, as e.g. a chromospheric activity and/or a disk around the primary component (see Sect. 7) contributing significantly to the global U luminosity.

Due to this problem, the calculation was made in two steps: first, a solution was obtained simultaneously on the *B1, B, B2, V1, V, G* light curves (thus without *U*) and the 2 radial velocity curves; second, with the obtained parameters, a solution including the *U* light curve was calculated.

The light curves for the seven filters are shown in Figs. 2 and 3. The quality of the fits is clearly very good, thus the values of the physical parameters obtained in this paper are secure. However, a slight asymmetry of the *U* light curve during the primary eclipse is noted (see Fig. 2), probably due to the characteristics of the *U* luminosity of the disk.

The values of the adjusted and calculated parameters are given in Tables 6 and 7. The following comments are to be made:

- The temperature T_2 is higher than the value determined in Sect. 4. Thus, the estimated spectral type of the secondary component appears to be close to G5III.
- The uncertainties on the calculated parameters are probably underestimated, because they are obtained for a fixed value of T_1. For that reason, in the following, the uncertainty on T_2 has been taken equal to 90 K (same value as the T_1 uncertainty).
- The value of the semi-major axis of the relative orbit $A = a_1 + a_2$ is $13.617 \pm 0.019\, R_\odot$ from the WD program (Table 6) and $13.40 \pm 0.06\, R_\odot$ from the orbital solution (Table 4). The difference between the two determinations corresponds to 2.7 times the sum of the uncertainties. This looks a bit too large, taking into account the quality of the data, but is nevertheless acceptable.
- A similar remark can be made for the mass ratio $q = M_2/M_1$ which takes the values 0.299 ± 0.008 from the radial velocity curves (see Sect. 5) and 0.2840 ± 0.0004 from the WD analysis (this section). This ratio was left as a free parameter to be adjusted in the photometric solution because the aim of this study is to find a solution from a simultaneous analysis of the light and radial velocity curves.
- The adjusted values of x_1 are in rather good agreement with the theoretical predictions of van Hamme (1993). Indeed, the adjusted (see Table 5) and theoretical values (for $T_1 = 9180$ and $\log g_1 = 3.97$) are respectively 0.775 ± 0.006 and 0.743 in *B*, 0.595 ± 0.007 and 0.636 in *V* (see Barblan et al. 1998 for a general comment on these discrepancies).
- Recall that the uncertainties on the derived parameters are of three types: i) Intrinsic, i.e. resulting from the mathematical analysis of the light and radial velocity curves (e.g. ±23 K on T_2); ii) Strongly correlated with the determination of *A* (e.g. the errors on $M_{1,2}$, $R_{1,2}$ and $\log g_{1,2}$); iii) Depending on the photometric determination of T_1 (e.g. the values of $M_{\rm bol}$).

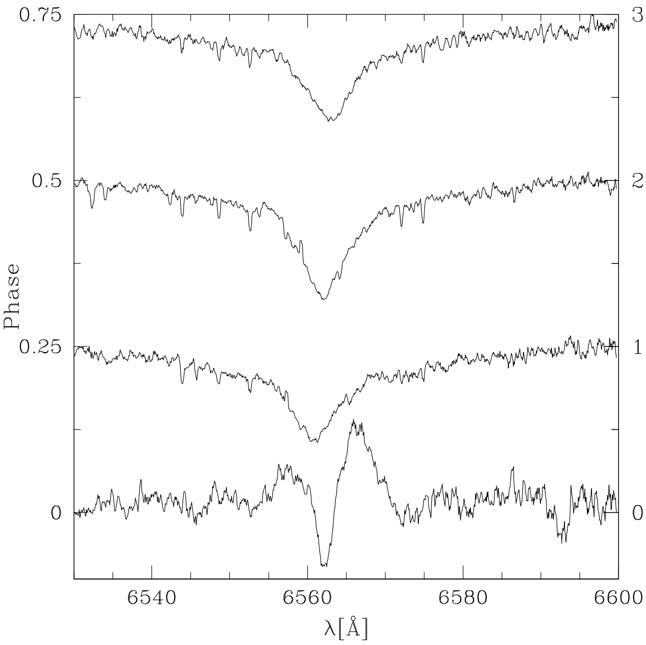

Fig. 4. Hα line profile at orbital phases 0.9995 (during the primary eclipse), 0.2288, 0.4939 (during the secondary eclipse) and 0.7382.

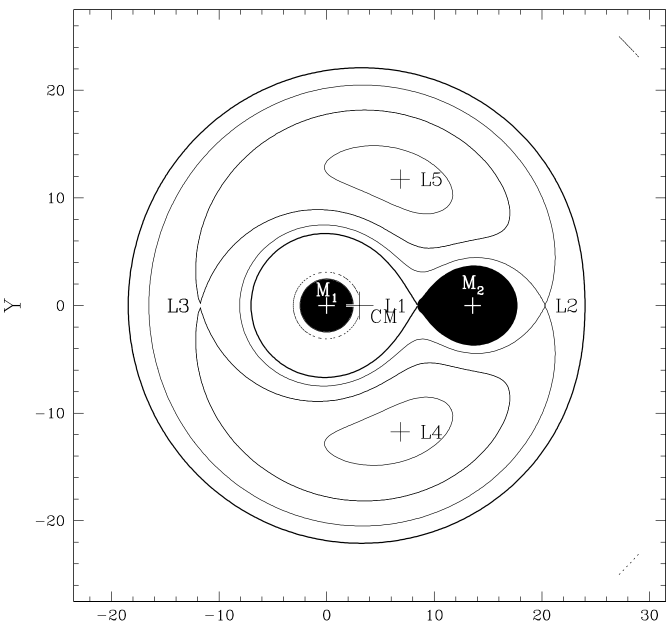

Fig. 5. Schematic view of the system in the equatorial plane (coordinates in $R_\odot$) of the BP Mus system. Some equipotential lines and the Lagrange points are indicated. The secondary star fills its Roche lobe.

7. Hα line profile variations

Figure 4 shows the profile of the Hα line at phase 0.9995 ± 0.0034 (exposure time 1980 s), i.e. during the primary eclipse, at phase 0.4939 ± 0.0031 (1760 s), i.e. during the secondary eclipse, and at intermadiate phases 0.2288 ± 0.0022 (1263 s) and 0.7382 ± 0.0031 (1800 s). As expected, the luminosity of the disk around the gainer hot primary star is large enough to produce the emission of the Hα line during the primary eclipse, when the primary component is eclipsed. From the ratio between $r_{\rm side_2}$ and $r_{\rm side_1}$, we deduce that the extension of the disk radius is larger than 1.4 R_1.

Note that the mass transfer from the secondary to the primary has been important in the history of BP Mus. Taking into account the present masses of the components, i.e. 2.40 $M_\odot$

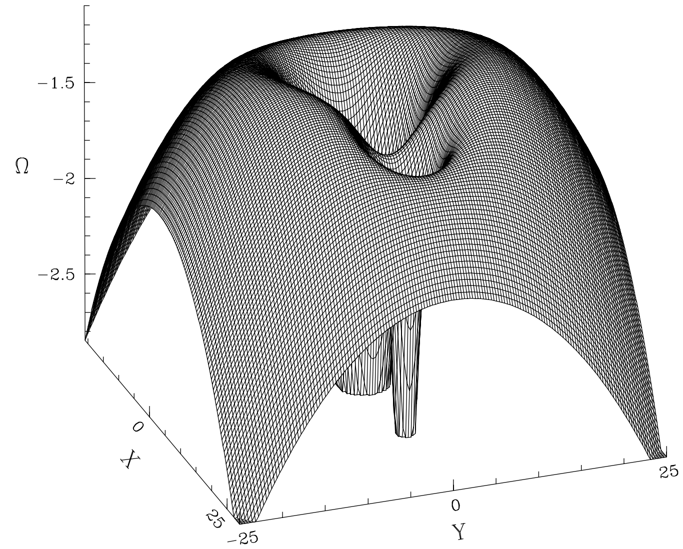

Fig. 6. Schematic view of the gravity potential Ω (see Sect. 7 for the definition) of the BP Mus system. The horizontal coordinates are in $R_\odot$.

and 0.68 $M_\odot$, the minimum value of this transfered mass is given by:

$$\Delta M = M_1 - (M_1 + M_2)/2 \simeq 0.86\ M_\odot.$$

8. Discussion and conclusion

Figures 5 and 6 present two views of BP Mus. Figure 5 is a "classical" representation of the two components in the equatorial plane. The 3-dimentional representation of the potential (Fig. 6) allows a better understanding of the meaning of the Lagrange points and of the path for the flow of the material from the secondary when it fills its Roche lobe. Recall that the L4 and L5 points are stable only in the case of a mass ratio $M_2/M_1 \leq 0.0385$ (Boccaletti & Pucacco 1996).

From the values of *V* (Table 2), $M_{\rm bol}$ (Table 7), *E[B2-V1]* and *[B2-V1]*$_0$ (Sect. 4), we derive a distance of 562 ± 17 pc for BP Mus, by adopting the value −0.025 ± 0.01 for the bolometric correction *BC* of the primary, according to the *BC*-colour relation of Flower (1977).

The simultaneous adjustment of the light curve model on high precision photometric data in seven passbands, ranging from 3400 to 6000 Å, puts strong constraints on the physical and orbital parameters of BP Mus. The essential results are presented in Figs. 2 and 3, Tables 6 and 7 and in the Abstract. The quality of the fits on the light curves and the uncertainties on the parameters show that this analysis has been successful.

The number of Algol-type binary systems for which the absolute parameters are determined on the basis of a self-consistent solution of both the light and radial velocity curves is very limited. There are now only 11 systems for which masses, radii and luminosities are known to accuracies typically better than 5%: the 9 systems mentioned by Maxted & Hilditch (1996), TZ Eri (Barblan et al. 1998) and BP Mus (this paper). In this context, it is important to enlarge the sample of very well known Algols, and this will be done in the near future with the analysis of 8 additional systems for which the photometric and spectroscopic campaings have been successful.

Acknowledgements. This work has been partly supported by the Swiss National Science Foundation. We are grateful to Prof. R. E. Wilson for the programme of analysis of the light curves, to Drs. P. North and E. C. Olson for many helpful comments and discussions, and to Prof. M. Mayor for the use of the spectrograph CORALIE. All graphs have been produced using the SuperMongo package (Lupton & Monger 1998).

References

Baranne, A., Queloz, D., Mayor, M., et al. 1996, A&AS, 119, 373
Barblan, F., Barthordi, P., North, P., Burki, G., & Olson, E. C. 1998, A&AS, 132, 367
Boccaletti, D., & Pucacco, G. 1996, Theory of Orbits, vol. 1 (Springer-Verlag, Berlin), 271
Burki, G., Kviz, Z., & North, P. 1992, A&A, 256, 463
Burnet, M., & Rufener, F. 1979, A&A, 74, 54
Flower, P. J. 1977, A&A, 54, 31
Golay, M. 1980, Vist. Astron. 24, 141
Golay, M., Peytremann, E., & Maeder, A. 1969, Publ. Obs. Genève, Série A, 76, 44
Hauck, B. 1994, ASP Conf. Ser., 60, 157
Hoffmeister, C. 1943, Kleinere Veröff. der Univ. (Berlin-Babelsberg), 27
Hubeny, I., Lanz, T., & Jeffery, C. S. 1994, TLUSTY and SYNSPEC: A User's Guide, Newsletter on Analysis of Astronomical Spectra, Univ. of St. Andrews
Kholopov, P. N., Samus, N. N., Frolov, M. S., et al. 1985, General Catalogue of Variable Stars (Nauka Publ. House, Moscow)
Kopal, Z. 1959, Close Binary Systems (Chapman, & Hall Ltd., London), 127
Künzli, M., North, P., Kurucz, R. L., & Nicolet, B. 1997, A&AS, 122, 51
Kupka, F., Piskunov, N. E., Ryabchikova, T. A., et al. 1999, A&AS, 138, 119
Kurucz, R. L. 1994, CD-ROM 19, Solar abundance atmosphere models for 0, 1, 2, 4, 8 km s^{-1}
Kviz, Z. 1986, I.B.V.S. 2863
Lupton, R. H., & Monger, P. 1998, SuperMongo Graphics and Computational Package (Princeton Astronomical Observatory and MacMaster University)
Maxted, P. F. L., & Hilditch, R. W. 1996, A&A, 311, 567
Nicolet, B. 1981a, A&A, 97, 85
Nicolet, B. 1981b, A&A, 104, 185
Queloz, D., Mayor, M., Udry, S., et al. 2001, The Messenger, 105, 1
Rufener, F. 1988, Catalogue of Stars Measured in the GENEVA Observatory Photometric System, 4th ed. (Obs. Genève)
Rufener, F., & Nicolet, B. 1988, A&A, 206, 357
Van Hamme, W. 1993, AJ, 106, 2096
Wilson, R. E. 1992, Documentation of Eclipsing Binary Computer Model (University of Florida, Gainesville)
Wilson, R. E., & Devinney, E. J. 1971, ApJ, 166, 605
Wilson, R. E., & Biermann, P. 1976, A&A, 48, 349